PHYSICAL REVIEW E **89**, 010902(R) (2014)

Effect of solvents on the pattern formation in a Belousov-Zhabotinsky reaction embedded into a microemulsion

Patricia Dähmlow,[1,*] Vladimir K. Vanag,[2] and Stefan C. Müller[1]

[1]*Institute of Experimental Physics, Otto-von-Guericke University Magdeburg, Universitätsplatz 2, 39106 Magdeburg, Germany*

[2]*Chemical-Biological Institute, Immanuel Kant Baltic Federal University, A. Nevskogo 14, 236041 Kaliningrad, Russia*

(Received 31 October 2013; published 30 January 2014)

Using the ferroin- and the bathoferroin-catalyzed Belousov-Zhabotinsky (BZ) reaction embedded in the sodium-bis (2-ethylhexyl) sulfosuccinate (AOT) water-in-oil microemulsion, we observed different patterns occurring in two different solvents, hexane and octane. Turing patterns were found in both solvents with ferroin. They differ in their interaction with coexisting bulk oscillations, such that a new excitation front was formed around the evolving Turing patterns in hexane. However, in octane, the bulk oscillation merged with the evolving patterns, forming a new excitation front, which propagated into two directions: towards the existing patterns and away from them. For the bathoferroin-catalyzed BZ reaction, patterns like dash waves, jumping waves, and bubble waves were found in both solvents having different wavelengths. A curvature dependence of the splitting and merging of dashes was found.

DOI: 10.1103/PhysRevE.89.010902 PACS number(s): 82.40.Ck, 89.75.Kd, 68.05.Gh, 82.33.Nq

I. INTRODUCTION

Pattern formation in activator-inhibitor systems presents an important phenomenon in biological morphogenesis, for instance, on animal skins [1]. These patterns are called Turing patterns, since they typically occur with a fast diffusing inhibitor and a slowly diffusing activator [2]. This is fulfilled in the Belousov-Zhabotinsky (BZ) reaction [3] incorporated in the ionic surfactant aerosol OT (AOT) [sodium bis(2-ethylhexyl)sulfosuccinate] reverse water-in-oil microemulsion (ME), if experiments are performed below the percolation transition. The reactants of the BZ reaction are dissolved in nanometer-sized water droplets (radius R [nm] $= 0.17\ \omega$, with $\omega = [H_2O]/[AOT]$, where $[H_2O]$ and [AOT] are the molar concentrations of H_2O and AOT, respectively) and diffuse with their velocity, if every water droplet behaves like a single droplet. The inhibitor, however, diffuses into the oil phase, leading to a diffusion constant about 10–100 times higher than that of the activator [4]. Above the percolation transition, a transient network of water channels is formed, leading to discontinuously propagating waves and dash waves [5,6].

The patterns occurring in the BZ-AOT ME depend on the chosen droplet fraction φ_d of a ME with $\varphi_d = (V_{AOT}+V_{H_2O})/V_{total}$, where V_{AOT}, V_{H_2O}, and V_{total} are the volumes of AOT, H_2O, and the total ME, respectively [4]. Percolation takes place around $\varphi_d \approx 0.5$ [5]. For $\varphi_d < 0.5$, stationary Turing patterns (spots and labyrinth structures) can be found, whereas above the percolation threshold, various types of wave patterns occur, like dash waves, which are wave fronts consisting of coherently moving wave segments separated by lateral gaps [5,7]. These dash waves evolve from a wave front by segmentation. A segment (dash) splits into two dashes when it reaches a certain length. With ferroin, dash waves occur only above the percolation transition, whereas with bathoferroin (BP), they can be found below and above the percolation transition [8].

Dash waves show, before segmentation of the front, an instability transverse to the wave front ("ripples"), which may occur through lateral inhibition or a kinetic interaction of the wave with a reactant in front of it. This instability, however, does not lead to a wave breakup with a slowly diffusing inhibitor, but with a fast diffusing one, a breakup of the wave front occurs [9–12]. The segmentation of wave fronts always starts near the center of a spiral, since the curvature is highest there. In the dashes, the inhibitor is primarily generated and, diffusing faster than the activator, suppressing the autocatalytic reaction in the neighboring gaps [7].

In this paper the differences of patterns in the ferroin- and bathoferroin-catalyzed BZ ME dissolved in octane or hexane are studied in the oscillatory regime of the reaction [13,14]. The patterns are observed for different ω. Using ferroin, a different Turing-Hopf type interaction is found for both solvents [15]. In the bathoferroin-catalyzed case, discontinuously propagating waves and dash waves are formed, differing in their wavelength for both solvents. Dash waves are found to split only if the curvature of the wave front is positive relative to the propagation direction (convex wave front), and they also show a merging of the dashes for a negative curvature (concave wave front).

II. MATERIALS AND METHODS

Experiments are performed by using the ferroin- or the bathoferroin-catalyzed BZ reaction dissolved in an AOT water-in-oil microemulsion. Octane and hexane (both from Sigma-Aldrich) are used as solvents.

The preparation of the stock solutions and of the microemulsion are described elsewhere [5,16]. φ_d is chosen very close to (but slightly below) the percolation transition. The concentrations of the reactants are listed in Tables I and II.

A small amount of the microemulsion is sandwiched between two glass plates with a Teflon spacer (thickness 80 μm, inner diameter 2.5 cm). The patterns developing in this reactor are illuminated by a LED panel through a 511 nm interference filter and observed through a microscope equipped

*patricia.daehmlow@ovgu.de

TABLE I. Concentrations of the reactants in the ferroin-catalyzed BZ-AOT system in octane and hexane for different ratios ω.

ω	Solvent	MA [M]	H_2SO_4 [M]	$NaBrO_3$ [M]	Ferroin [mM]	φ_d
12	Octane	0.25	0.175	0.15	4.2	0.455
	Hexane	0.3	0.2		4	
15	Both	0.247	0.197	0.177	4.41	0.468
18	Both	0.259	0.207	0.155	4.14	0.43
20	Both	0.3	0.2	0.15	4	0.485

with a digital CCD camera connected to a computer. All experiments are carried out at temperature 25±1 °C.

The electrical conductivity is measured with the conductivity meter YSI model 3200 by starting with an initial droplet fraction φ_d between 0.68 and 0.74 of the reactive microemulsion and adding the solvent gradually until reaching a conductivity below 1 μS/cm.

The measured images of the patterns are analyzed in IDL (Interactive Data Language, ITT Visual Information Solutions). First, a contrast improvement is done. The binarization of the images is done by using the function "MORPH_GRADIENT," which is the subtraction of an eroded version from a dilated version of the original image. Afterwards, a threshold for the binarization is chosen.

The characteristic wavelength of the Turing patterns is calculated by using the spatial FFT. The curvature of a wave front is calculated by placing three points along the wave front. From these three points a circle is calculated, whose radius is the inverse curvature of the wave front.

III. RESULTS

A. Ferroin-catalyzed BZ reaction

The conductivity of the ME with hexane as the solvent is shown exemplarily in Fig. 1(a), since the conductivities in hexane and octane are almost equal. The conductivity remains below 1 μS/cm for $\varphi_d = 0.4$-0.5 (our typical experimental range) and $\omega = 15$–22, while for $\omega = 12$, the conductivity is significantly increased. Thus, for $\omega > 15$, experiments are below the percolation transition, but for $\omega = 12$, percolation starts in the chosen range of φ_d. The same holds for bathoferroin as the catalyst.

The characteristic Turing wavelength λ and the dynamical behavior of the observed patterns are almost equal in a series of experiments with identical initial conditions, but the particular shape of patterns can be different. ω is changed from 12 to 20 for both solvents, and the concentrations of the reactants

TABLE II. Concentrations of the reactants in the bathoferroin-catalyzed BZ-AOT system in octane and hexane for different ω. The recipes are equal for both solvents.

ω	MA [M]	H_2SO_4 [M]	$NaBrO_3$ [M]	BP [mM]	φ_d
12	0.242	0.174	0.194	6	0.455
15	0.243	0.175	0.194	4.87	0.36
20	0.242	0.174	0.194	3.8	0.485

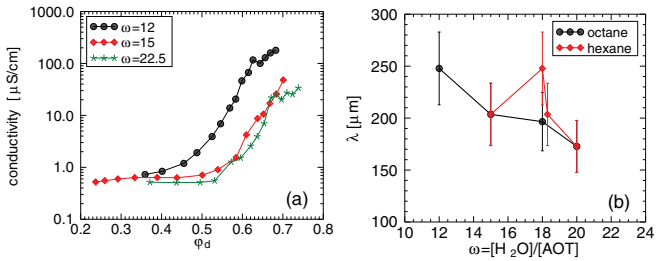

FIG. 1. (Color online) (a) Conductivity of the BZ-AOT microemulsion dissolved in hexane as a function of φ_d; (b) characteristic Turing wavelength λ in octane and hexane for different ω. For recipes see Table I.

are varied slightly (Table I). The wavelength λ is shown in Fig. 1(b) for different ω and $\varphi_d = 0.43$–0.485. It lies around 200 μm in octane and hexane, decreasing with increasing ω. Also the period of the bulk oscillations is almost equal for octane and hexane. It varies strongly only for the different chosen ω, lying in the range between 102 and 284 ± 2 s.

In experiments with $\omega > 12$ and φ_d around 0.45, Turing patterns can be found. The interaction between the bulk oscillations and the stationary Turing patterns differs in both solvents (Fig. 2). In octane, the oscillation does not extinguish the evolving Turing patterns, but it merges with the existing front. This front gets thin and a moment later it drifts apart, such that one part propagates into the direction away from and the other part towards the emerging Turing patterns [arrows in Fig. 2(a)]. The front propagating towards the inner circles, later forms the labyrinth structure with the growing structures inside the rings.

However, in hexane bulk oscillation forms a new ring around the evolving Turing patterns. The oscillation (in the form of fast phase wave) stops at a distance a little smaller than the characteristic wavelength of the system, and the medium between the oscillatory part and the existing patterns remains in the reduced state. After the medium returns to the reduced state, the ring formed by the oscillation remains [Fig. 2(b)]. This type of the development of Turing patterns is called "frozen waves" [17], although this name was used earlier for precipitation waves in the BZ reaction [18].

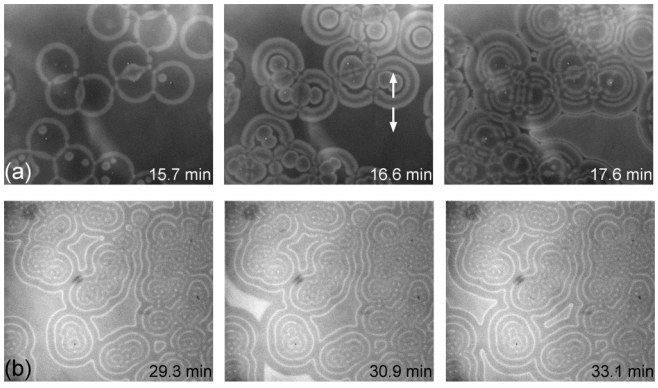

FIG. 2. Snapshots of Turing patterns with $\omega = 18.03$ ($\varphi_d = 0.43$) at different instants of time in octane (a) and in hexane [19] (b). For recipes see Table I (size of snapshots: 5.3 × 4.6 mm^2).

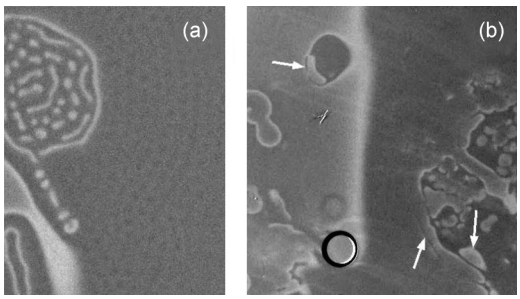

FIG. 3. Patterns in the ferroin-catalyzed BZ-AOT microemulsion with $\omega = 12$, $\varphi_d = 0.455$ at $t = 38.9$ min (a) in octane (size: 2.77×3.61 mm^2) and (b) in hexane (size: 2.47×2.64 mm^2) [19]. The white arrows in (b) point to jumping waves, and the black circle is a gas bubble. For recipes see Table I.

For experiments with $\omega = 12$ in hexane, no Turing patterns can be observed, but discontinuously propagating waves like jumping waves are found [Fig. 3(b)], whereas in octane, Turing patterns form [Fig. 3(a)]. Despite the slightly different recipes, φ_d is the same (0.455) and the conductivity of 1 μS/cm indicates that the system is close to the percolation transition. The bulk oscillations are nonuniform in both octane and hexane. In octane, this can be seen at the reduced space in the lower left corner of Fig. 3(a). The oscillation forms a new stationary ring around the emerging Turing patterns, but breaks up in the course of the experiment forming stationary Turing spots. These spots fluctuate around their point of origin, until they remain stationary, such that there is an almost equal distance between all Turing spots.

In hexane, the bulk oscillations do not excite the medium homogeneously either. Some regions are surrounded by the oscillation and excited a short moment later by jumping waves [see upper left arrow in Fig. 3(b)]. These waves omit small stripes of the medium, which remain in the reduced state for a little longer than the surrounding medium.

B. Bathoferroin-catalyzed BZ reaction

In the bathoferroin-catalyzed system, dash waves or spirals, as well as discontinuously propagating waves, such as rotating and jumping waves evolve (Fig. 4). In both solvents the occurring patterns are similar except the wavelength, which is larger in octane than in hexane.

In octane a pacemaker occurs due to a small impurity at the beginning of the measurement. Towards it, dash waves propagate from the upper left corner [Fig. 4(c)]. The patterns produced by the pacemaker develop from target patterns into rotating waves, which occur in front of the outer wave front. The rotating wave turns around this front, until it encompasses it. Then, the next wave occurs in front of this wave. With time, these waves propagate slowly away from the pacemaker, since they disappear after they occupy the medium. Later, rotating waves develop into bubble waves [Fig. 4(a)]. When those discontinuously propagating waves approach the dash waves, they propagate much slower and stop before reaching the dash wave front. Therefore, the originally circular shape produced by the pacemaker disappears.

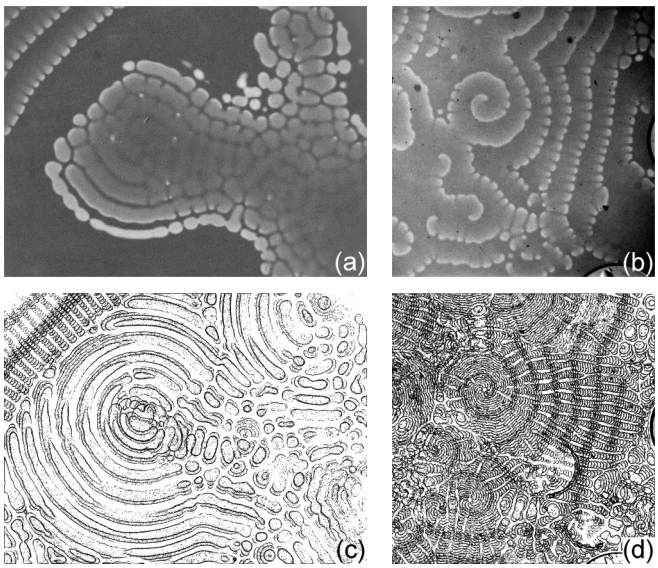

FIG. 4. Snapshots of patterns in the bathoferroin-catalyzed BZ reaction with $\omega = 12$ ($\varphi_d = 0.455$) at $t = 224.8$ min (a) in octane (size of images: 8.1×6.1 mm^2) and (b) in hexane (size of images: 5.9×6.1 mm^2) [19]. Superposition of binarized images (c) in octane between 180.0 min and 189.2 min and (d) in hexane between 220.0 and 227.9 min with time interval of 40 s. For recipes see Table II. Note that the black lines in the superposition represent the oxidized state of the reaction.

For the same recipe with hexane, also dash waves are found. Exemplarily a spiral wave is shown, whose wave fronts are segmented [Fig. 4(b)]. Interestingly, the dashes of one wave front propagate into the gaps of the previous one; i.e., the fronts are displaced relative to their precursor by the length of a dash [Figs. 4(c) and 4(d)].

The length of the dashes vary between 90 and 163 ± 2 μm and the length of the gaps vary from 40 to 104 ± 2 μm in both solvents for different ω, respectively. The ratio between the length of the dashes and the length of the gaps range between 2.1 and 2.4 ± 0.1 in the different experiments.

For convex waves a splitting of dashes can be observed. Therefore, the length of the dashes immediately before splitting is 1.7 to 1.9 ± 0.1 times larger than the length of normal dashes. The segmentation begins near the core of the spiral or at the inner wave front produced by a pacemaker, since the curvature of the wave fronts is larger there than at the outer fronts.

The frequency distribution of the curvature is shown in Fig. 5. For a mean curvature, the number of splitting dashes is much higher than that for small or large curvatures, since large curvatures occur only near the spiral core, where the number of dashes is much smaller than at the outer wave fronts.

A splitting of the dashes can only be observed for convex wave fronts, where the dashes propagate away from each other. For a concave curvature [as in Fig. 4(a)] a merging of dashes can be found. The gaps get smaller, such that the dashes move closer together until they merge. Splitting or merging of the dashes cannot be observed for a curvature K between -0.10 and 0.21 ± 0.1 mm^{-1}; i.e., for almost plain

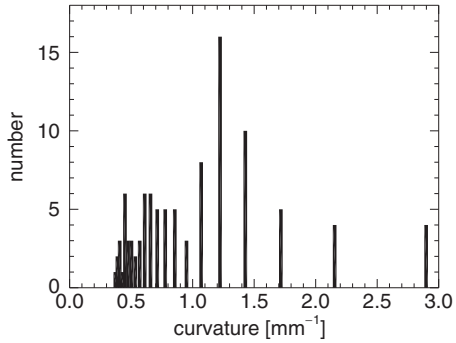

FIG. 5. Frequency distribution of the curvature K of a wave front, at which a splitting of the dashes occur ($\omega = 12$, hexane).

wave fronts, the dashes propagate straightforward without changing their length.

IV. DISCUSSION

The interaction of bulk oscillations with stationary Turing patterns in the ferroin-catalyzed BZ-AOT system dissolved in octane seems to resemble the phase diffusion waves studied in Ref. [20], where a perturbation leads to a trigger wave. Also this interaction is a result of Turing-Hopf interaction that can lead to different spatiotemporal patterns like oscillatory Turing patterns; see, for example, Refs. [15,21].

However, the Turing-Hopf type interactions differs for the solvents used in our experiments, which may be due to an effect of different viscosities and of different partition coefficients for the activator ($HBrO_2$; $P_{act} = [HBrO_2]_{oil}/[HBrO_2]_{droplet}$) and the inhibitor Br_2 in both solvents. The partition coefficient for Br_2 between water and octane is 0.5 [22]. For hexane no value for this coefficient was found. If the coefficients P_{act} and/or P_{inh} change with the solvent, different patterns can emerge in different solvents, as observed for the BZ-microdroplets in a microfluidic device [23]. The ratio P_{act}/P_{inh} can affect the pattern formation in a quite similar manner as the ratio between diffusion coefficients.

When using bathoferroin, dash waves and discontinuously propagating waves are observed. A corresponding phase diagram of patterns found in the BZ-AOT system is shown in Ref. [6]. The change of patterns in the bathoferroin-catalyzed system may be due to the more hydrophobic character of the catalyst (BP is not soluble in water). Its molecules are located mostly in the hydrophobic AOT shell, yielding a clustering of nanodroplets. This effect can be seen by dynamical light scattering, where peaks at 50–100 nm occur, which are absent or extremely small with ferroin.

The occurring dash waves propagate in a similar way as waves studied in Refs. [24,25]. In particular, the behavior of free wave fronts depending on the local excitability of the medium are found to increase or shorten their length [26].

Here the segmentation of wave fronts begin near the spiral core, since the curvature of the wave front is highest there. Due to the convex wave front, the dash waves have rapidly enough lateral space to reach their splitting length. With decreasing curvature, the number of splitting dashes decreases. The curvature K, where the most frequent splitting occurred, is $1.22 \pm 0.2\ \mathrm{mm}^{-1}$; independently of the oil and the shape of the dominant pattern. The segmentation is found not to depend on the front velocity, since its change (which is a function of K), is smaller than 5% of the velocity of a plane wave. Therefore, the curvature $K = O(1)$ [27] (approximated with a diffusion coefficient of the activator of $10^{-7}\ \mathrm{cm}^2\ \mathrm{s}^{-1}$) [4].

The displacement of the dashes between wave fronts may occur due to the primarily generation of the inhibitor in the dashes [7], since this trace is not yet excitable, when the next wave front reaches it.

In this study, the mechanism for two different hydrocarbon solvents affecting pattern formation is suggested. This was previously thought not to be important for pattern formation. Furthermore, in microemulsions, long-range interactions can be expected to occur due to the percolation. This can be observed in Fig. 2(b), where the bulk oscillation stops, before emerging Turing patterns. Also with bathoferroin, this type of interactions is observed [Fig. 4(a)], since rotating waves and bubble waves propagate much slower towards the dash wave front than into the other directions. This underlines the complexity of the studied system, making it thus an interesting model case for complexity, in particular for biological morphogenesis. Indeed, the BZ-AOT system is full of surprises.

ACKNOWLEDGMENTS

P. D. thanks the Graduiertenförderung des Landes Sachsen-Anhalt for financial support. Valuable discussions with Henning Scheich and Frank Ohl, as well as technical assistance by Veronika Zelentsova, are gratefully acknowledged.

[1] S. Kondo and T. Miura, Science **329**, 1616 (2010).
[2] A. M. Turing, Phil. Trans. R. Soc. Lond. B **237**, 37 (1952).
[3] A. N. Zaikin and A. M. Zhabotinsky, Nature **225**, 535 (1970).
[4] L. J. Schwartz, C. L. DeCiantis, S. Chapman, B. K. Kelley, and J. P. Hornak, Langmuir **15**, 5461 (1999).
[5] V. K. Vanag and I. R. Epstein, Proc. Natl. Acad. Sci. USA **100**, 14635 (2003).
[6] V. K. Vanag, Physics-Uspekhi **47**, 923 (2004).
[7] V. K. Vanag and I. R. Epstein, Phys. Rev. Lett. **90**, 098301 (2003).
[8] A. A. Cherkashin, V. K. Vanag, and I. R. Epstein, J. Phys. Chem. **128**, 204508 (2008).
[9] D. Horváth, V. Petrov, S. K. Scott, and K. Showalter, J. Chem. Phys. **98**, 6332 (1993).
[10] Y. Kuramoto and H. Arakai, *Chemical Oscillations, Waves and Turbulence* (Springer, Berlin, 1984).
[11] M. Markus, G. Kloss, and I. Kusch, Nature (London) **371**, 402 (1994).

[12] V. S. Zykov, A. S. Mikhailov, and S. C. Müller, Phys. Rev. Lett. **81**, 2811 (1998).
[13] J. Ross, S. C. Müller, and C. Vidal, Science **240**, 460 (1988).
[14] A. Zhabotinsky and A. Zaikin, J. Theor. Biol. **40**, 45 (1973).
[15] A. De Wit, D. Lima, G. Dewel, and P. Borckmans, Phys. Rev. E **54**, 261 (1996).
[16] V. K. Vanag and I. R. Epstein, Phys. Rev. Lett. **87**, 228301 (2001).
[17] I. R. Epstein, V. K. Vanag, A. C. Balazs, O. Kuksenok, P. Dayal, and A. Bhattacharya, Acc. Chem. Res. **45**, 2160 (2012).
[18] J. M. Köhler and S. C. Müller, J. Phys. Chem. **99**, 980 (1995).
[19] See Supplemental Material at http://link.aps.org/supplemental/10.1103/PhysRevE.89.010902 for details on the Turing patterns and on the dash waves.
[20] J. M. Bodet, J. Ross, and C. Vidal, J. Chem. Phys. **86**, 4418 (1987).
[21] J. Carballido-Landeira, V. K. Vanag, and I. R. Epstein, Phys. Chem. Chem. Phys. **12**, 3656 (2010).
[22] M. Toiya, H. O. González-Ochoa, V. K. Vanag, S. Fraden, and I. R. Epstein, J. Phys. Chem. Lett. **1**, 1241 (2010).
[23] V. K. Vanag and I. R. Epstein, Phys. Rev. E **84**, 066209 (2011).
[24] T. Sakurai, E. Mihaliuk, F. Chirila, and K. Showalter, Science **296**, 2009 (2002).
[25] Z. Nagy-Ungvarai, A. M. Pertsov, B. Hess, and S. C. Müller, Physica D **61**, 205 (1992).
[26] Z. Nagy-Ungvarai and S. C. Müller, Int. J. Bifurcat. Chaos **04**, 1257 (1994).
[27] J. J. Tyson and J. P. Keener, Physica D **32**, 327 (1988).